

# Molecular Origin of Photoprotection in Cyanobacteria Probed by Watermarked Femtosecond Stimulated Raman Spectroscopy

Yusaku Hontani,<sup>†,⊥</sup> Miroslav Kloz,<sup>‡,⊥</sup> Tomáš Polívka,<sup>§,⊥</sup> Mahendra K. Shukla,<sup>||</sup> Roman Sobotka,<sup>||</sup> and John T. M. Kennis<sup>\*,†,⊥</sup>

<sup>†</sup>Department of Physics and Astronomy, Vrije Universiteit, De Boelelaan 1081, 1081 HV Amsterdam, The Netherlands

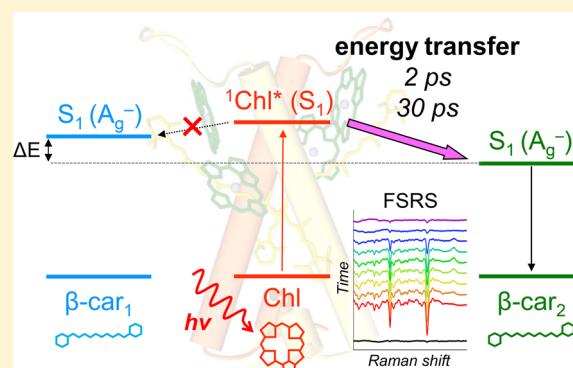
<sup>‡</sup>ELI-Beamlines, Institute of Physics, Na Slovance 2, 182 21 Praha 8, Czech Republic

<sup>§</sup>Institute of Physics and Biophysics, Faculty of Science, University of South Bohemia, 370 05 České Budějovice, Czech Republic

<sup>||</sup>Centre Algatech, Institute of Microbiology, Academy of Sciences of the Czech Republic, Třeboň, 379 81, Czech Republic

## Supporting Information

**ABSTRACT:** Photoprotection is fundamental in photosynthesis to avoid oxidative photodamage upon excess light exposure. Excited chlorophylls (Chl) are quenched by carotenoids, but the precise molecular origin remains controversial. The cyanobacterial HliC protein belongs to the Hlip family ancestral to plant light-harvesting complexes, and binds Chl *a* and  $\beta$ -carotene in 2:1 ratio. We analyzed HliC by watermarked femtosecond stimulated Raman spectroscopy to follow the time evolution of its vibrational modes. We observed a 2 ps rise of the C=C stretch band of the  $2A_g^-$  ( $S_1$ ) state of  $\beta$ -carotene upon Chl *a* excitation, demonstrating energy transfer quenching and fast excess-energy dissipation. We detected two distinct  $\beta$ -carotene conformers by the C=C stretch frequency of the  $2A_g^-$  ( $S_1$ ) state, but only the  $\beta$ -carotene whose  $2A_g^-$  energy level is significantly lowered and has a lower C=C stretch frequency is involved in quenching. It implies that the low carotenoid  $S_1$  energy that results from specific pigment–protein or pigment–pigment interactions is the key property for creating a dissipative energy channel. We conclude that watermarked femtosecond stimulated Raman spectroscopy constitutes a promising experimental method to assess energy transfer and quenching mechanisms in oxygenic photosynthesis.



Oxygenic photosynthetic organisms need to protect themselves from the consequences of excess sunlight, as the photosynthetic machinery easily gets overloaded even at moderate light intensities. To this end, elaborate photoprotection mechanisms have evolved, collectively known as nonphotochemical quenching (NPQ).<sup>1,2</sup> NPQ involves the active dissipation (quenching) of singlet excited states in the light harvesting antenna before they reach the reaction centers for photochemical conversion, and manifests itself in distinct ways in various oxygenic photosynthetic organisms. In plants and algae, NPQ involves specific interactions between carotenoids and chlorophylls in the light-harvesting complex (LHC) family, where the lifetime of Chl singlet excited states is quenched to hundreds of picoseconds. The mechanism by which this process occurs has been controversially discussed in the literature:<sup>3</sup> energy transfer,<sup>4–8</sup> electron transfer,<sup>9–11</sup> excitonic coupling,<sup>12,13</sup> and Chl–Chl charge transfer interactions<sup>14</sup> have been proposed.

Cyanobacterial photosynthesis is ancestral to that of plants and algae, and although cyanobacteria do not use the plant-like LHC antenna system for light harvesting, they contain so-called high-light inducible proteins (Hlips) that are homologues to first and third helices of plant LHC proteins. Hlips are small

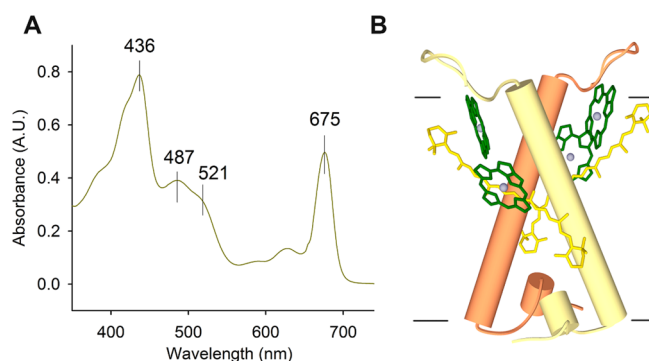
single-helix polypeptides (5–7 kDa) ubiquitous in cyanobacteria, which play an important role during assembly and repair of photosystem II, particularly under stress conditions.<sup>15</sup> So far, only two members of the Hlip family, HliC and HliD, have been isolated and biochemically characterized.<sup>5,16</sup> Both these proteins, isolated from the cyanobacterium *Synechocystis* 6803, form oligomers, and bind four Chl *a* (HliC) or six Chl *a* (HliD) and 2  $\beta$ -carotenes per a putative dimer.<sup>5,16</sup>

Figure 1 shows the absorption spectrum and a structural model of HliC.<sup>5</sup> Despite the apparent 2-fold symmetry in the proposed structure, resonance Raman spectroscopy demonstrated that two distinct  $\beta$ -carotene conformers exist in HliC and also in HliD:<sup>17</sup>  $\beta$ -car<sub>1</sub> absorbs at higher energy and exhibits a higher C=C stretch frequency at 1525 cm<sup>-1</sup>, whereas  $\beta$ -car<sub>2</sub> absorbs at lower energy and has a lower C=C stretch frequency at 1515 cm<sup>-1</sup>. Strikingly, ultrafast transient absorption spectroscopy showed that the HliD protein was highly quenched, with dominant Chl *a* lifetimes of only 2 and 30 ps, and a minor unquenched fraction.<sup>5</sup> Moreover, it was

Received: March 2, 2018

Accepted: March 23, 2018

Published: March 23, 2018

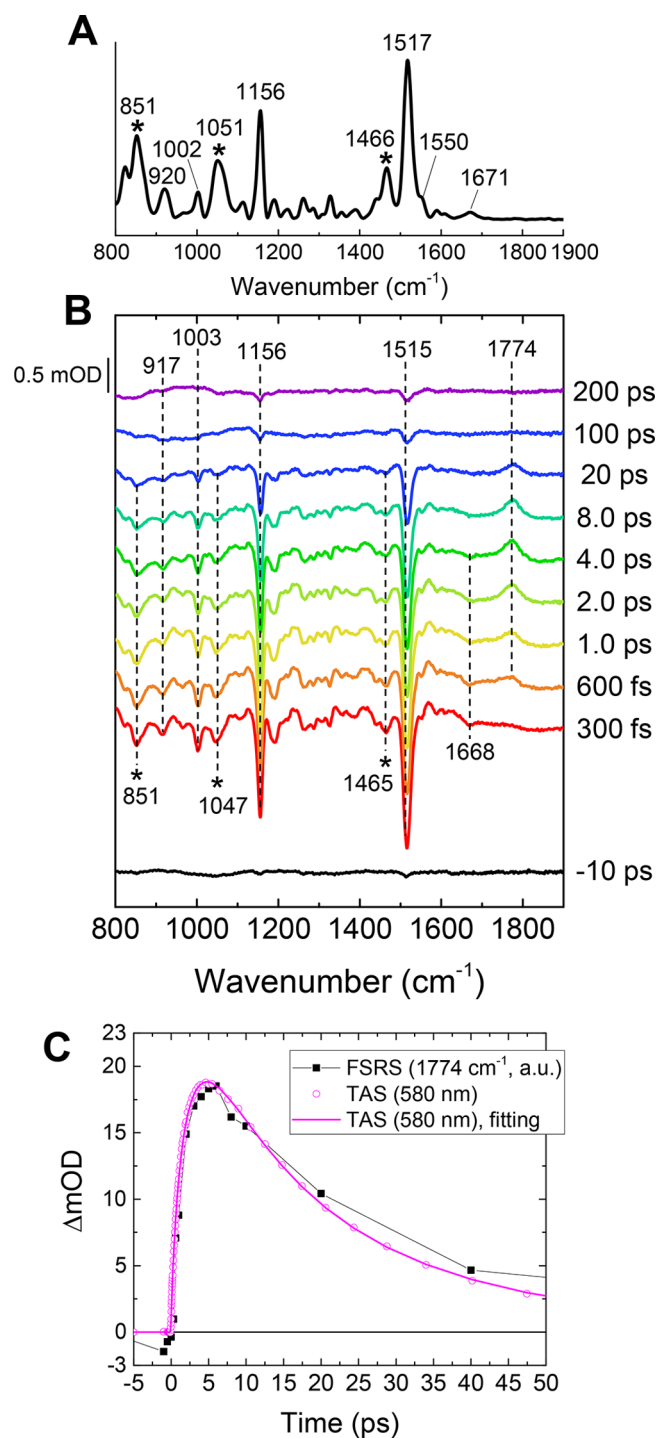


**Figure 1.** Steady-state absorption and a structural model of HliC. (A) Room-temperature absorbance spectrum of the purified HliC protein. (B) Structural model of the putative HliC dimer depicted as a side view along the membrane plane (modified from ref 16).

shown that the quenching of the Chl *a* excited state proceeded via energy transfer to the optically forbidden  $S_1$  ( $A_g^-$ ) state of  $\beta$ -carotene.<sup>5</sup> This observation posed an important conundrum: close Chl-carotenoid positioning that is a common motif in light-harvesting proteins is necessary to promote triplet–triplet transfer from Chl to carotenoid upon Chl intersystem crossing. Yet, in most antenna complexes, the Chl singlet excited state is not quenched at all. Hence, unresolved questions remain about the quenching mechanisms in photosynthetic light harvesting complexes with regard to electronic coupling to optically forbidden states and the energetics of the states involved.<sup>18</sup> The latter is especially pressing because the energy level of the optically forbidden  $S_1$  state of carotenoids is largely insensitive to polarity and polarizability of the environment.<sup>19</sup>

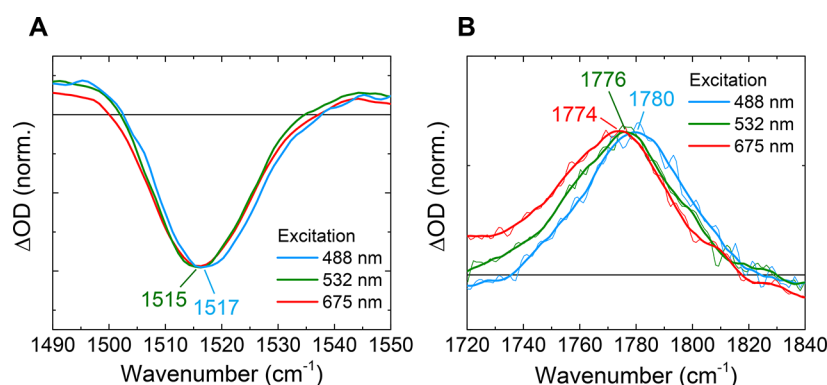
Femtosecond stimulated Raman spectroscopy (FSRS) is a powerful method to gain detailed molecular information through transient vibrational spectra.<sup>20</sup> It features a high temporal resolution of <100 fs, high spectral resolution, and high sensitivity with respect to time-resolved resonance Raman methods. Recently, we have developed a watermarked FSRS method involving shot-to-shot Raman pump wavelength modulation and wavelet transformation to successfully suppress the large and unpredictable baseline fluctuations that have dogged the FSRS method since its inception more than a decade ago.<sup>21–23</sup> Through this method, baseline issues due to nonresonant nonlinear contributions, transient absorption, pump–dump–probe, and pump–repump probe signals are successfully suppressed without any biased human intervention. Watermarked FSRS seems particularly suited to study pigment–protein complexes of oxygenic photosynthesis since its Raman pump at 800 nm is conveniently preresonant with the main pigment absorption bands. In this work, we make use of the ability of FSRS to follow specific molecular vibrations with sub-100 fs time resolution to assess the mechanism, pathways, and energetics of excited-state energy quenching in HliC. To our knowledge, this work represents the first demonstration of energy transfer processes in a photosynthetic light harvesting complex probed with FSRS and lays the groundwork for general application of the watermarked FSRS method in photosynthesis research.

Figure 2A shows the stimulated Raman spectrum of the HliC ground state with preresonant 800 nm pump. The two strongest bands at 1517 and 1156  $\text{cm}^{-1}$  are due to the  $\beta$ -carotene C=C ( $\nu_1$ ) and C–C stretches ( $\nu_2$ ), respectively.<sup>16,17</sup> The bands at 1002 and 920  $\text{cm}^{-1}$  belong to the  $\nu_3$  (methyl in-



**Figure 2.** FSRS of HliC upon 675 nm excitation. (A) Ground-state Raman spectrum of HliC. (B) Selected time traces of difference spectra of FSRS. Asterisks (\*) indicate signals originated from glycerol. (C) Transient absorption kinetic trace at 580 nm (magenta open dots) with a fitting curve (magenta line) overlapped with FSRS data at 1774  $\text{cm}^{-1}$  (black closed squares).

plane rocking) and  $\nu_4$  (hydrogen-out-of plane rocking) vibrations of  $\beta$ -carotene, respectively.<sup>16,17</sup> It furthermore features a shoulder near 1550  $\text{cm}^{-1}$  and a band at 1671  $\text{cm}^{-1}$ , which are both due to Chl *a*.<sup>16</sup> The amplitude of the  $\beta$ -carotene bands is much higher than those of Chl *a* even though the 800 nm Raman pump is more preresonant with the Chl *a*  $Q_y$  band than the  $\beta$ -carotene  $S_2$  band, which relates to the higher Raman



**Figure 3.** Comparison of FSRS bands of HliC at 4 ps upon excitation at different wavelengths. (A) The bleaches of the C=C stretch in the ground state and (B) the C=C stretch of the  $S_1$  state of  $\beta$ -carotene. Signals upon excitation at 488, 532, and 675 nm are shown in cyan, green, and red, respectively. In panel B, a 21 point smoothing (over  $1\text{ cm}^{-1}$  intervals) was applied (thick lines) with Savitzky–Golay filtering. The thin lines show the watermarked data without smoothing.

cross section of the latter pigment. The bands at 1466, 1051, and  $851\text{ cm}^{-1}$  are due to glycerol, which was added to stabilize the sample and are conveniently used as an internal marker for the FSRS experiments. The spectral width of the HliC stimulated Raman bands is approximately  $20\text{ cm}^{-1}$ , which is larger than the bandwidth expected from convolution with the spectral width of the Raman pump ( $\sim 10\text{ cm}^{-1}$ ). Hence, the observed bandwidths do not result from the experimental conditions but are inherent to the HliC protein at room temperature.

Figure 2B shows FSRS spectra at selected delays upon Chl *a* excitation at 675 nm. At very short delays (300 fs), large bleaches of the  $\beta$ -carotene C=C stretch at  $1515\text{ cm}^{-1}$  and C–C stretch at  $1156\text{ cm}^{-1}$  are observed, as well as a bleach of the Chl *a* band at  $1668\text{ cm}^{-1}$ . Importantly, the glycerol solvent bands at 1465, 1047, and  $851\text{ cm}^{-1}$  are bleached as well, which indicates that these are likely spurious signals caused by partial absorption of the 800 nm Raman pump by Chl *a* excited-state absorption (ESA),<sup>24,25</sup> i.e., an inner filter effect that diminishes the Raman pump intensity and hence results in a lower signal.<sup>26</sup> Thus, the bleaching signals associated with  $\beta$ -carotene stretches at early delay times do not imply population of  $\beta$ -carotene excited states. This was confirmed by a FSRS experiment on a Chl *a*– $\beta$ -carotene mixture in organic solvent, where no close interactions exist between the pigments. Here, selective Chl *a* excitation and population also lead to bleach of Chl *a*,  $\beta$ -carotene, and solvent modes (Figure S1), confirming the inner filter effect. We did not observe any positive bands that arise from the Chl *a* excited state, which may seem surprising given the resonance of the Raman pump with the Chl *a* ESA. However, the Chl *a* ESA has a rather low amplitude, and the strong electronic transition to the  $Q_y$  state at 670 nm, which is preresonant with the Raman pump in the ground state, entirely disappears in the excited state. At the same time,  $\beta$ -carotene has a very high Raman cross section. Apparently, these combined effects result in Chl *a* excited-state Raman bands that are unobservably weak with respect to those of the  $\beta$ -carotene ground state.

In the ensuing evolution on the picosecond time scale, we observe the rise of a positive band at  $1774\text{ cm}^{-1}$ . This band is a unique marker of the optically forbidden  $S_1$  ( $2A_g^-$ ) state of carotenoids, as it represents an upshifted C=C stretch frequency that results from strong vibronic coupling between the  $S_0$  ( $1A_g^-$ ) and  $S_1$  ( $2A_g^-$ ) states.<sup>27</sup> Thus, FSRS data gives direct evidence of energy transfer from the excited Chl *a* to the

optically forbidden  $S_1$  state of  $\beta$ -carotene in 2 ps, consistent with transient absorption measurements (Figures 2C, S2, and S3) where the  $\beta$ -carotene  $S_1$  state has a prominent absorption at 560 nm. The same quenching pathway has also been earlier reported by ultrafast transient absorption experiments on HliD.<sup>5</sup> The  $1774\text{ cm}^{-1}$  band disappears on a time scale of 10 ps, which is assigned to the  $S_1$ – $S_0$  internal conversion (IC) of  $\beta$ -carotene.<sup>19</sup> In addition, a minor slow phase of 30 ps is observed in the  $\beta$ -carotene  $S_1$  decay ( $1774\text{ cm}^{-1}$ ) in transient absorption as well as in stimulated Raman. The Chl *a* bleach signal mainly decayed in 2.5 and 20 ps (Figure S2). Given that the IC time constant of  $\beta$ -carotene can hardly be longer than 15 ps due to the properties of its conjugated  $\pi$ -electron system,<sup>19</sup> we interpret this to result from a slow 30 ps phase in the energy transfer process from Chl *a* to  $\beta$ -carotene, which through inverted kinetics (i.e., when a state is populated slower than it is depopulated, it rises with its decay time, and decays with its rise time) shows up as a 30 ps lifetime component of the  $\beta$ -carotene  $S_1$  state. A nondecaying phase in the Chl *a* transient absorption is assigned to a minor fraction of loosely bound or unbound Chl *a* (Figure S2B, magenta line).

Given the (low) Chl *a* ESA around 800 nm, it might be anticipated that Chl *a* could be promoted to a higher-up excited state due to the combined actions of actinic and Raman pumps. However, the FSRS time evolution closely follows that of the TA experiments (Figures 2C and S3), indicating that such processes, if they occur at all, do not affect the FSRS experiment in any appreciable way.

To gain additional information about the energy transfer processes and pathways, we performed FSRS experiments with direct excitation of  $\beta$ -carotene at 488 and 532 nm (Figure S4). Here, the two  $\beta$ -carotene conformers,  $\beta$ -car<sub>1</sub> and  $\beta$ -car<sub>2</sub>, are to a certain extent selectively excited. We observe that, for both data sets upon 488- and 532 nm excitation, the high-frequency  $\beta$ -carotene  $S_1$  marker band around  $1775\text{ cm}^{-1}$  rises in about 300 fs and upshifts with approximately the same time constant, which is assigned to ultrafast IC from the optically allowed  $S_2$  state, followed by intramolecular vibrational cooling.<sup>21,28</sup> For both data sets, the  $\beta$ -carotene  $S_1$  marker band decays in  $\sim 10$  ps. Figure S5 shows the results of transient absorption experiments with 488 and 532 nm excitation.

Although the spectral evolution is very similar between the two data sets, significant spectral differences are observed. Figure 3 shows an overlap of the FSRS spectra at 4 ps in the C=C stretch regions of the  $S_0$  state (panel A) and  $S_1$  state

(panel B) with excitation at 488 nm (cyan), 532 nm (green), and 675 nm (red). Strikingly, in the  $S_1$  state (Figure 3B) a 4  $\text{cm}^{-1}$  difference in the band maxima is observed with 488 and 532 nm excitation, which demonstrates that the  $\beta\text{-car}_1$  and  $\beta\text{-car}_2$  conformers have distinct C=C stretch frequencies in the  $S_1$  state. Note that selectivity is not 100% with either excitation wavelength,<sup>17</sup> so the difference in  $S_1$  state frequency of  $\beta\text{-car}_1$  and  $\beta\text{-car}_2$  is probably larger than 4  $\text{cm}^{-1}$ . Smaller, but observable shifts were observed in the ground state C=C stretch manifested as the  $S_0$  state bleaching signal (Figure 3A). Figure S6 shows overlapped FSRS spectra at various time delays.

If we now compare the FSRS data with Chl *a* excitation at 675 nm (Figure 3B, red) with that at 488 nm excitation (Figure 3B, cyan), we find that the former has a frequency of 1774  $\text{cm}^{-1}$ , which is lower by 6  $\text{cm}^{-1}$  than the latter (Figure 3B). This observation demonstrates that the  $\beta\text{-car}_2$  conformer, and not  $\beta\text{-car}_1$  acts as the energy acceptor that quenches the excited Chl *a*. In HliC and HliD, on the basis of the linear relationship between the ground state C=C stretch frequency and effective conjugation length,<sup>29</sup> the conjugation length of  $\beta\text{-car}_2$  was estimated to be  $\sim 10.5$ , as opposed to  $\sim 9.6$  for  $\beta\text{-car}_1$ ,<sup>16</sup> which would result in an up to 800  $\text{cm}^{-1}$  (0.1 eV) energy difference between  $\beta\text{-car}_1$  and  $\beta\text{-car}_2$ .<sup>19</sup> The 6  $\text{cm}^{-1}$  shift of the C=C stretch frequency in the  $S_1$  state observed here by FSRS corroborates this finding, although the precise relationship between the C=C stretch frequency in the  $S_1$  state and effective conjugation has not been established yet. The  $S_1$  C=C frequency of carotenoids is determined through the combined effects of the effective  $\pi$ -electron conjugation length and the vibronic coupling with the  $S_0$  state.<sup>27</sup> Under the assumption that the vibronic coupling with  $S_0$  is the same for  $\beta\text{-car}_1$  and  $\beta\text{-car}_2$ , this result implies that the  $S_1$  energy of  $\beta\text{-car}_2$  indeed is lower than that of  $\beta\text{-car}_1$ . This finding implies that specific carotenoid–protein interactions induces asymmetry between the  $\beta$ -carotene molecules in HliC, making the  $\beta\text{-car}_2$  the quenching site.

Figure 4 summarizes our findings. Application of FSRS allowed to follow the specific vibrational mode in the  $S_1$  state, revealing that the  $\beta$ -carotene  $S_1$  energy level tuning provides a key property in creating dissipative energy transfer pathways in closely confined Chl–carotenoid geometries. The carotenoid  $S_1$

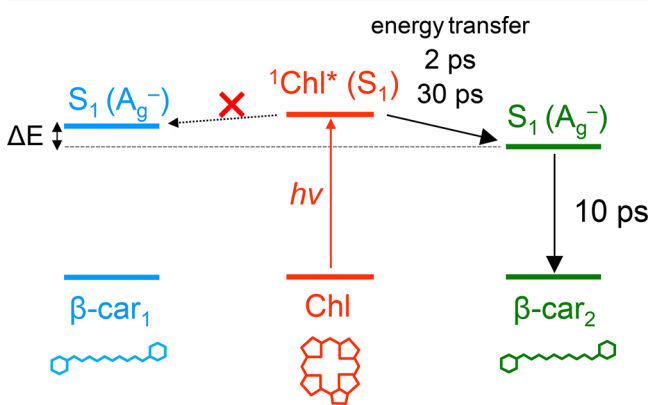


**Figure 4.** Energy transfer model of HliC upon excitation of Chl. After excitation of Chl, excited-state energy transfer occurs specifically to the lower energy  $\beta$ -carotene ( $\beta\text{-car}_2$ ) in 2 and 30 ps. The decay of the  $S_1$  state  $\beta\text{-car}_2$  proceeds in 10 ps. The higher-energy  $\beta\text{-car}_1$  is not populated because of unfavorable energetics. See text for details.

state energy is largely insensitive to environmental polarity and polarizability,<sup>19</sup> which implies that specific pigment–protein or pigment–pigment interactions must be invoked to tune the  $S_1$  energy. One promising avenue is provided by specific in-plane tuning of the  $\beta$ -carotene  $\beta$ -rings, which bring them in conjugation with the  $\pi$ -electron system of the polyene backbone, thereby lowering the overall energy levels of the electronic excited states.<sup>17</sup> The ramifications of these observations are very important indeed, as the same type of carotenoid molecule,  $\beta$ -carotene in this case, may assume a quenching and a nonquenching role in the same Hlip, a mechanism that has long been hypothesized for plant LHCs.<sup>2,4,30</sup> Here, watermarked FSRS has revealed the vibrational signature of the  $\beta$ -carotene quenching state in HliC, and the technique may play an important role in elucidating quenching mechanisms in various types of LHCs that are less clear-cut and harder to assess by traditional means.

## ■ ASSOCIATED CONTENT

### Supporting Information

The Supporting Information is available free of charge on the ACS Publications website at DOI: 10.1021/acs.jpcllett.8b00663.

Additional experimental details, global fitting analysis, and transient absorption spectra (PDF)

## ■ AUTHOR INFORMATION

### Corresponding Author

\*E-mail: j.t.m.kennis@vu.nl

### ORCID

Tomáš Polívka: 0000-0002-6176-0420

John T. M. Kennis: 0000-0002-3563-2353

### Author Contributions

<sup>†</sup>Y.H. and M.K. contributed equally.

### Notes

The authors declare no competing financial interest.

## ■ ACKNOWLEDGMENTS

Y.H. and J.T.M.K. were supported by the Chemical Sciences Council of The Netherlands Organization for Scientific Research (NWO) through a VICI grant and a Middelgroot investment grant to J.T.M.K. M.K. was supported by the Czech Science Foundation project number 17-01137S. R.S. and M.K.S. were supported by the project 17-08755S of the Czech Science Foundation and by the Czech Ministry of Education (project LO1416). T.P. was supported by the project P501/12/G055 from the Czech Science Foundation.

## ■ REFERENCES

- (1) Croce, R.; van Amerongen, H. Natural Strategies for Photosynthetic Light Harvesting. *Nat. Chem. Biol.* **2014**, *10*, 492–501.
- (2) Ruban, A. V.; Johnson, M. P.; Duffy, C. D. P. Natural Light Harvesting: Principles and Environmental Trends. *Energy Environ. Sci.* **2011**, *4*, 1643–1650.
- (3) van Oort, B.; Roy, L. M.; Xu, P. Q.; Lu, Y. H.; Karcher, D.; Bock, R.; Croce, R. Revisiting the Role of Xanthophylls in Non-photochemical Quenching. *J. Phys. Chem. Lett.* **2018**, *9*, 346–352.
- (4) Ruban, A. V.; Berera, R.; Ilioaia, C.; van Stokkum, I. H. M.; Kennis, J. T. M.; Pascal, A. A.; van Amerongen, H.; Robert, B.; Horton, P.; van Grondelle, R. Identification of a Mechanism of Photoprotective Energy Dissipation in Higher Plants. *Nature* **2007**, *450*, 575–578.
- (5) Staleva, H.; Komenda, J.; Shukla, M. K.; Slouf, V.; Kana, R.; Polívka, T.; Sobotka, R. Mechanism of Photoprotection in the

Cyanobacterial Ancestor of Plant Antenna Proteins. *Nat. Chem. Biol.* **2015**, *11*, 287–291.

(6) Berera, R.; Herrero, C.; van Stokkum, I. H. M.; Vengris, M.; Kodis, G.; Palacios, R. E.; van Amerongen, H.; van Grondelle, R.; Gust, D.; Moore, T. A.; et al. A Simple Artificial Light-Harvesting Dyad as a Model for Excess Energy Dissipation in Oxygenic Photosynthesis. *Proc. Natl. Acad. Sci. U. S. A.* **2006**, *103*, 5343–5348.

(7) Berera, R.; van Grondelle, R.; Kennis, J. T. M. Ultrafast Transient Absorption Spectroscopy: Principles and Application to Photosynthetic Systems. *Photosynth. Res.* **2009**, *101*, 105–118.

(8) Liguori, N.; Xu, P. Q.; van Stokkum, I. H. M.; van Oort, B.; Lu, Y. H.; Karcher, D.; Bock, R.; Croce, R. Different Carotenoid Conformations Have Distinct Functions in Light-Harvesting Regulation in Plants. *Nat. Commun.* **2017**, *8*, 1994.

(9) Holt, N. E.; Zigmantas, D.; Valkunas, L.; Li, X. P.; Niyogi, K. K.; Fleming, G. R. Carotenoid Cation Formation and the Regulation of Photosynthetic Light Harvesting. *Science* **2005**, *307*, 433–436.

(10) Ahn, T. K.; Avenson, T. J.; Ballottari, M.; Cheng, Y. C.; Niyogi, K. K.; Bassi, R.; Fleming, G. R. Architecture of a Charge-Transfer State Regulating Light Harvesting in a Plant Antenna Protein. *Science* **2008**, *320*, 794–797.

(11) Park, S.; Fischer, A. L.; Li, Z. R.; Bassi, R.; Niyogi, K. K.; Fleming, G. R. Snapshot Transient Absorption Spectroscopy of Carotenoid Radical Cations in High-Light-Acclimating Thylakoid Membranes. *J. Phys. Chem. Lett.* **2017**, *8*, 5548–5554.

(12) Bode, S.; Quentmeier, C. C.; Liao, P. N.; Hafi, N.; Barros, T.; Wilk, L.; Bittner, F.; Walla, P. J. On the Regulation of Photosynthesis by Excitonic Interactions between Carotenoids and Chlorophylls. *Proc. Natl. Acad. Sci. U. S. A.* **2009**, *106*, 12311–12316.

(13) Kloz, M.; Pillai, S.; Kodis, G.; Gust, D.; Moore, T. A.; Moore, A. L.; van Grondelle, R.; Kennis, J. T. M. Carotenoid Photoprotection in Artificial Photosynthetic Antennas. *J. Am. Chem. Soc.* **2011**, *133*, 7007–7015.

(14) Muller, M. G.; Lambrev, P.; Reus, M.; Wientjes, E.; Croce, R.; Holzwarth, A. R. Singlet Energy Dissipation in the Photosystem II Light-Harvesting Complex Does Not Involve Energy Transfer to Carotenoids. *ChemPhysChem* **2010**, *11*, 1289–1296.

(15) Komenda, J.; Sobotka, R. Cyanobacterial High-Light-Inducible Proteins - Protectors of Chlorophyll-Protein Synthesis and Assembly. *Biochim. Biophys. Acta, Bioenerg.* **2016**, *1857*, 288–295.

(16) Shukla, M. K.; Llansola-Portoles, M. J.; Tichy, M.; Pascal, A. A.; Robert, B.; Sobotka, R. Binding of Pigments to the Cyanobacterial High-Light-Inducible Protein HliC. *Photosynth. Res.* **2017**, DOI: 10.1007/s11120-017-0475-7.

(17) Llansola-Portoles, M. J.; Sobotka, R.; Kish, E.; Shukla, M. K.; Pascal, A. A.; Polivka, T.; Robert, B. Twisting a beta-Carotene, an Adaptive Trick from Nature for Dissipating Energy during Photoprotection. *J. Biol. Chem.* **2017**, *292*, 1396–1403.

(18) Balevicius, V.; Fox, K. F.; Bricker, W. P.; Jurinovich, S.; Prandi, I. G.; Mennucci, B.; Duffy, C. D. P. Fine Control of Chlorophyll-Carotenoid Interactions Defines the Functionality of Light-Harvesting Proteins in Plants. *Sci. Rep.* **2017**, *7*, 13956.

(19) Polivka, T.; Sundstrom, V. Ultrafast Dynamics of Carotenoid Excited States - From Solution to Natural and Artificial Systems. *Chem. Rev.* **2004**, *104*, 2021–2071.

(20) Kukura, P.; McCamant, D. W.; Mathies, R. A. Femtosecond Stimulated Raman Spectroscopy. *Annu. Rev. Phys. Chem.* **2007**, *58*, 461–488.

(21) Kloz, M.; Weissenborn, J.; Polivka, T.; Frank, H. A.; Kennis, J. T. M. Spectral Watermarking in Femtosecond Stimulated Raman Spectroscopy: Resolving the Nature of the Carotenoid S\* State. *Phys. Chem. Chem. Phys.* **2016**, *18*, 14619–14628.

(22) Kloz, M.; van Grondelle, R.; Kennis, J. T. M. Wavelength-Modulated Femtosecond Stimulated Raman Spectroscopy - Approach towards Automatic Data Processing. *Phys. Chem. Chem. Phys.* **2011**, *13*, 18123–18133.

(23) Hontani, Y.; Inoue, K.; Kloz, M.; Kato, Y.; Kandori, H.; Kennis, J. T. M. The Photochemistry of Sodium Ion Pump Rhodopsin Observed by Watermarked Femto- to Submillisecond Stimulated

Raman Spectroscopy. *Phys. Chem. Chem. Phys.* **2016**, *18*, 24729–24736.

(24) Nuijs, A. M.; Shuvalov, V. A.; Van Gorkom, H. J.; Plijter, J. J.; Duysens, L. N. M. Picosecond Absorbency Difference Spectroscopy on the Primary Reactions and the Antenna-Excited States in Photosystem-I Particles. *Biochim. Biophys. Acta, Bioenerg.* **1986**, *850*, 310–318.

(25) Zigmantas, D.; Hiller, R. G.; Sundstrom, V.; Polivka, T. Carotenoid to Chlorophyll Energy Transfer in the Peridinin-Chlorophyll-a-Protein Complex Involves an Intramolecular Charge Transfer State. *Proc. Natl. Acad. Sci. U. S. A.* **2002**, *99*, 16760–16765.

(26) Kloz, M.; van Grondelle, R.; Kennis, J. T. M. Correction for the Time Dependent Inner Filter Effect Caused by Transient Absorption in Femtosecond Stimulated Raman Experiment. *Chem. Phys. Lett.* **2012**, *544*, 94–101.

(27) Nagae, H.; Kuki, M.; Zhang, J. P.; Sashima, T.; Mukai, Y.; Koyama, Y. Vibronic Coupling Through the In-phase, C=C Stretching Mode Plays a Major role in the 2A(g)(-) to 1A(g)(-) Internal Conversion of All-Trans-Beta-Carotene. *J. Phys. Chem. A* **2000**, *104*, 4155–4166.

(28) McCamant, D. W.; Kukura, P.; Mathies, R. A. Femtosecond Time-Resolved Stimulated Raman Spectroscopy: Application to the Ultrafast Internal Conversion in Beta-Carotene. *J. Phys. Chem. A* **2003**, *107*, 8208–8214.

(29) Mendes-Pinto, M. M.; Sansiaume, E.; Hashimoto, H.; Pascal, A. A.; Gall, A.; Robert, B. Electronic Absorption and Ground State Structure of Carotenoid Molecules. *J. Phys. Chem. B* **2013**, *117*, 11015–11021.

(30) Pandit, A.; Reus, M.; Morosinotto, T.; Bassi, R.; Holzwarth, A. R.; de Groot, H. J. M. An NMR Comparison of the Light-Harvesting Complex II (LHCII) in Active and Photoprotective States Reveals Subtle Changes in the Chlorophyll a Ground-State Electronic Structures. *Biochim. Biophys. Acta, Bioenerg.* **2013**, *1827*, 738–744.